

Controlling the anomalous Hall effect by electric-field-induced piezo-strain in $\text{Fe}_{40}\text{Pt}_{60}/(001)\text{-Pb}(\text{Mg}_{1/3}\text{Nb}_{2/3})_{0.67}\text{Ti}_{0.33}\text{O}_3$ multiferroic heterostructures

Cite as: Appl. Phys. Lett. 112, 033506 (2018); <https://doi.org/10.1063/1.5008591>

Submitted: 08 October 2017 • Accepted: 03 January 2018 • Published Online: 18 January 2018

 Yuanjun Yang, Yingxue Yao, Lei Chen, et al.



View Online



Export Citation



CrossMark

ARTICLES YOU MAY BE INTERESTED IN

[Reversible electrical-field control of magnetization and anomalous Hall effect in Co/PMN-PT hybrid heterostructures](#)

Applied Physics Letters **112**, 152904 (2018); <https://doi.org/10.1063/1.5022381>

[Opportunities and challenges for magnetoelectric devices](#)

APL Materials **7**, 080905 (2019); <https://doi.org/10.1063/1.5112089>

[Piezostain control of anomalous Hall resistivity of \$\[\text{Co}/\text{Pt}\]_3\text{-Pb}\(\text{Mg}_{1/3}\text{Nb}_{2/3}\)\text{O}_3\text{-PbTiO}_3\$ heterostructure](#)

AIP Advances **10**, 045318 (2020); <https://doi.org/10.1063/5.0003928>



Time to get excited.
Lock-in Amplifiers – from DC to 8.5 GHz

[Find out more](#)

 Zurich Instruments

Controlling the anomalous Hall effect by electric-field-induced piezo-strain in $\text{Fe}_{40}\text{Pt}_{60}/(001)\text{-Pb}(\text{Mg}_{1/3}\text{Nb}_{2/3})_{0.67}\text{Ti}_{0.33}\text{O}_3$ multiferroic heterostructures

Yuanjun Yang,^{1,a)} Yingxue Yao,¹ Lei Chen,² Haoliang Huang,³ Benjian Zhang,¹ Hui Lin,¹ Zhenlin Luo,³ Chen Gao,³ Y. L. Lu,³ Xiaoguang Li,⁴ Gang Xiao,^{5,a)} Ce Feng,⁶ and Y. G. Zhao⁶

¹*School of Electronic Science and Applied Physics, and Laboratory of Quantum Materials and Interfaces, Hefei University of Technology, Hefei, Anhui 230009, People's Republic of China*

²*School of Materials Science and Engineering, Hefei University of Technology, Hefei 230009, People's Republic of China*

³*National Synchrotron Radiation Laboratory, University of Science and Technology of China, Hefei, Anhui 230026, People's Republic of China*

⁴*Hefei National Laboratory for Physical Sciences at the Microscale and Department of Physics, University of Science and Technology of China, Hefei, Anhui 230026, People's Republic of China*

⁵*Department of Physics, Brown University, Providence, Rhode Island 02912, USA*

⁶*Department of Physics and State Key Laboratory of Low-Dimensional Quantum Physics, Tsinghua University, Beijing 100084, People's Republic of China*

(Received 8 October 2017; accepted 3 January 2018; published online 18 January 2018)

Electric-field control of the anomalous Hall effect (AHE) was investigated in $\text{Fe}_{40}\text{Pt}_{60}/(001)\text{-Pb}(\text{Mg}_{1/3}\text{Nb}_{2/3})_{0.67}\text{Ti}_{0.33}\text{O}_3$ (FePt/PMN-PT) multiferroic heterostructures at room temperature. It was observed that a very large Hall resistivity change of up to 23.9% was produced using electric fields under a magnetic field bias of 100 Oe. A pulsed electric field sequence was used to generate nonvolatile strain to manipulate the Hall resistivity. Two corresponding nonvolatile states with distinct Hall resistivities were achieved after the electric fields were removed, thus enabling the encoding of binary information for memory applications. These results demonstrate that the Hall resistivity can be reversibly switched in a nonvolatile manner using programmable electric fields. Two remanent magnetic states that were created by electric-field-induced piezo-strain from the PMN-PT were attributed to the nonvolatile and reversible properties of the AHE. This work suggests that a low-energy-consumption-based approach can be used to create nonvolatile resistance states for spintronic devices based on electric-field control of the AHE. *Published by AIP Publishing.* <https://doi.org/10.1063/1.5008591>

One of the benefits of spintronics is low power consumption. For this purpose, there has been active research in the manipulation of magnetic states using an electric field (EF). Here, the magnetic states include in-plane and perpendicular magnetic anisotropies in thin films,¹ magnetic domain wall (DW) propagation,² magnetic phase transitions,³ and magnetic exchange interaction.⁴ Additionally, EF control of the Hall effect offers a new prospect for the applications of spintronics, particularly, in magnetic memory devices. Insulated-gate field-effect transistor structures have been used to control the Hall effect to sense the magnetic states of some multilayers.^{5–7} However, the short charge-penetration depth cannot control the magnetic states inside ferromagnetic films effectively.⁸ Increasing the EF strength is not an option due to the potential breakdown of gate dielectrics.⁹ Another approach to the EF control of magnetic properties is to rely on the interfacial mechanical strain coupling between a ferromagnetic and a ferroelectric film in multiferroic hybrid structures.^{10–13} This method is much more effective because one can select highly responsive ferromagnetic (via piezomagnetism) and ferroelectric components.^{14,15} Carman *et al.* reported strain-mediated domain

wall (DW) rotation in ferromagnetic Ni rings formed on $\text{Pb}(\text{Mg}_{1/3}\text{Nb}_{2/3})_{0.66}\text{Ti}_{0.34}\text{O}_3$ single crystals.¹⁵ An experimental demonstration of a complete 180° reversal of magnetization was also produced in nanomagnetic $\text{Co}/\text{Pb}(\text{Mg}_{1/3}\text{Nb}_{2/3})_{0.7}\text{Ti}_{0.3}\text{O}_3$ multiferroic heterostructures via strain-mediated magnetoelectric coupling.¹⁶ Qiu *et al.* were able to electrically switch the magnetic vortex circulation in an artificial multiferroic $\text{Co}/\text{Cu}/\text{PMN-PT}$ structure.¹³

Indeed, in recent years, there has been increasing research into EF control of the Hall effect using multiferroic heterostructures.^{7,17–19} Wang *et al.* observed that EF control of the anomalous Hall effect (AHE) can enable the direct probing of magnetization reversal in heavy metal/ferromagnetic structures composed of $\text{Pt}/\text{Co}/\text{Ni}/\text{Co}/\text{Pt}$ layers on PMN-PT substrates.¹⁷ The AHE was also modulated by EF-induced strain in multiferroic $\text{Ni}_{43}\text{Mn}_{41}\text{Co}_5\text{Sn}_{11}/\text{PMN-PT}$ heterostructures,¹⁸ indicating the possibility of an additional degree of freedom in the design of spintronic devices through EF control of the Hall effect. EF control of the AHE was also reported in $\text{Pt}/\text{Bi}_{0.9}\text{La}_{0.1}\text{FeO}_3$ multiferroic heterostructures.⁷ However, in these studies, the EF control of AHE was volatile, which limits its utility in spintronics.¹⁷ Nonvolatile control of the AHE within the framework of strain-mediated multiferroic structures has not been fully explored to date.

^{a)}Authors to whom correspondence should be addressed: yangyuanjun@hfut.edu.cn and gang_xiao@brown.edu.

However, heavy metal/ferromagnetic structures, such as those based on Pt/Co/Ni/Co/Pt layers, $(\text{Co/Pt})_n$, and $(\text{Fe/Pt})_n$ multilayers or alloys of Fe, Co, and Pt, have been studied extensively because of their controllable magnetic anisotropy and spin reorientation properties.^{14,20} Xiao *et al.* observed that the AHE is more than three orders of magnitude higher than the normal Hall effect in $\text{Fe}_x\text{Pt}_{100-x}$ and $\text{Co}_x\text{Pt}_{100-x}$ thin films, indicating that they are good candidate materials for spintronic applications.^{21,22} Yu *et al.* fabricated L1_0 -FePt thin films on NiTi shape memory alloy substrates and achieved nonvolatile modulation of the magnetic anisotropy and magnetization reversal characteristics of these films.²⁰ Deterministic switching of the perpendicular magnetic anisotropy using electric fields was also demonstrated in $(\text{Co/Pt})_3/\text{Pb}(\text{Mg}_{1/3}\text{Nb}_{2/3})\text{O}_3$ - PbTiO_3 multiferroic heterostructures.¹⁴

In this work, with the motivation of realizing EF control of the magnetic effects and the giant Hall effect in Fe-Pt alloys, all-electrical programmable manipulations of AHE were studied in $\text{Fe}_{40}\text{Pt}_{60}/(001)\text{-Pb}(\text{Mg}_{1/3}\text{Nb}_{2/3})_{0.67}\text{Ti}_{0.33}\text{O}_3$ (FePt/PMN-PT) multiferroic heterostructures. We have observed that AHE can be reversibly switched in a nonvolatile manner using a sequence of pulsed electric fields at room temperature. We will explain these switching results based on the strain-mediated magnetoelectric coupling mechanism.

One Pt target and one Fe target were used to deposit the thin films on glass substrates ($\sim 50\ \mu\text{m}$ thick) via high-vacuum magnetron sputtering techniques. We were able to achieve the desired compositions and thicknesses by precise control of the sputtering rates and times on each target. The FePt thin film thickness used in this work was approximately 30 nm. Full details of the thin film growth process can be found in Refs. 22 and 23. Standard lift-off optical lithography procedures yielded the Hall bar structures, which have $150 \times 1300\ \mu\text{m}^2$ main channels. We used the standard four-probe technique to perform transport measurements at room temperature while taking suitable precautions to eliminate any errors caused by thermoelectric voltages and Hall probe misalignment. The multiferroic heterostructure was subsequently fabricated by epoxy bonding of the polarized (001)- $\text{Pb}(\text{Mg}_{1/3}\text{Nb}_{2/3})_{0.67}\text{Ti}_{0.33}\text{O}_3$ single crystal to the Cr/Au electrodes and the glass substrate.²⁴ After the epoxy had fully cured, the Hall bar devices were then installed on a probe station with *in situ* magnetic fields that were generated using a pair of electromagnets.²⁵ The strain versus electric field curves were then measured by the strain gauge method, as demonstrated in our previous work.^{26,27}

Figure 1(a) shows a schematic illustration of the FePt/PMN-PT multiferroic heterostructures. The positive electric field is defined in the direction from the bottom electrode to the top electrode, as indicated by the dotted arrows. The external magnetic field \mathbf{H} is applied perpendicular to the Hall bar structure. The positive magnetic field is directed upwards, as indicated by the bold arrow. The Hall channel lies along the [100] direction of the PMN-PT single crystal. An optical image of the Hall bar is shown in Fig. 1(b). R_{xy} is the Hall resistance, which is determined based on the Hall voltage and the applied current I_s . The Hall resistivity ρ_H is then calculated while considering the FePt channel thickness. One typical calculation result is plotted in Fig. 1(c). The Hall resistivity of the FePt thin film was $1.09 \times 10^{-7}\ \Omega\ \text{cm}$ after positive full polarization, which is consistent with previously reported

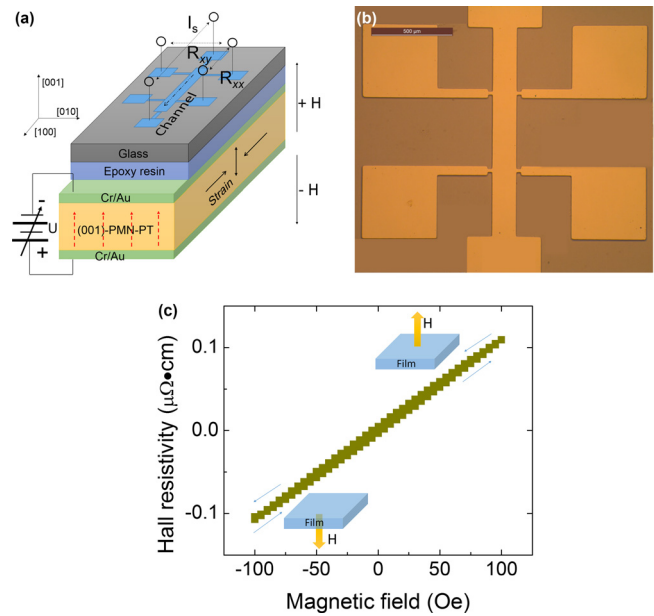


FIG. 1. (a) Schematic of the FePt/PMN-PT multiferroic heterostructure. (b) An optical image of the Hall bar. (c) A typical Hall resistivity curve shown as a function of the sweeping magnetic fields. The insets show the FePt Hall bar and the magnetic field configuration in accordance with (a).

values.^{21–23} The FePt thin films in this work have an A1-type structure with a face-centered cubic (fcc) symmetry as shown in Fig. S1 (for more details, see [supplementary material](#)).

It is well known that electric-field control of the magnetic properties of materials is a result of strain-mediated magnetoelectric coupling.^{1,9–11} We must therefore turn to a study of the strain states, which are transferred from the PMN-PT substrate to the FePt thin film through the converse piezoelectric effect. First, the cycle of applied electric fields in the continuous mode shown in Fig. 2(a) was used to measure the strain along the [100] direction of the PMN-PT. This method has been commonly used in the literature.^{26–28} The corresponding results are plotted in Fig. 2(b). The observed butterfly-like behavior can be expected when using this mode. Consequently, there was no remanent strain upon removal of the applied electric fields.²⁶ Second, a sequence of electric fields in the pulsed mode shown in Fig. 2(c) was used to perform the strain measurements, in the manner reported by Zhao *et al.*²⁸ In both modes, the strain was measured at the end of the interval, as indicated by the arrows in both Figs. 2(a) and 2(c). The difference between these modes is that the electric voltage (field) is constantly applied to the PMN-PT in the continuous mode, whereas no electric voltage (field) is applied during the interval in the pulsed mode. In the pulsed mode, the strain is actually measured under zero electric field bias and thus reflects the remanent strain states within the PMN-PT substrate. The resulting strain versus electric field curve is presented in Fig. 2(d) and shows bipolar loop-like behavior. Removal of the pulsed electric field from $+5.5\ \text{kV/cm}$ to a zero field sets the remanent strain state “A,” and removal of the pulsed electric field from $-5.5\ \text{kV/cm}$ to a zero field sets up another remanent strain state “B.” These two distinct remanent strain states are both stable, indicating the possibility of control of the nonvolatile Hall effect using electric fields. It is generally recognized that the magnetoelectric coupling effect through strain

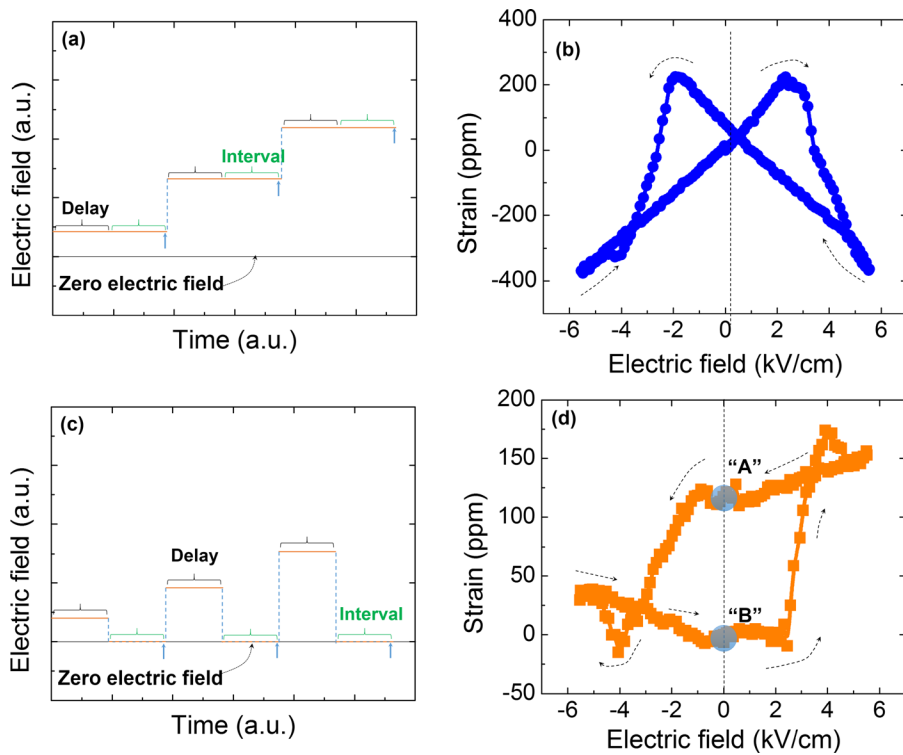


FIG. 2. (a) and (c) Schematic diagrams of the continuous and pulsed modes used for the strain-electric-field curve measurements, respectively. The strain measurement begins at the end of the interval indicated by the arrows in each case. (b) and (d) Corresponding in-plane strain vs. electric field curves for the continuous and pulsed modes, respectively. The dotted lines with arrows show the cycling directions of the electric fields.

transfer from the ferroelectric layer to the ferromagnetic layer will induce a remarkable modulation in magnetic anisotropy.^{1,4,9} Hence, the electric-field-control of the AHE in the FePt/PMN-PT heterostructures can be realized indirectly via strain-mediated magnetoelectric coupling. Here, the remanent strain state “B” is referenced as having a value of 0 ppm. The remanent strain state “A” is then given a strain value of up to +120 ppm, which is of the same order of magnitude as that in Ref. 28 (ca. $\sim +400$ ppm). It should also be mentioned that the strain is tensile after depolarization from +5.5 kV/cm to the zero field, which is in agreement with previously reported results.²⁸ This behavior is closely related to the ferroelectric polarization switching of the PMN-PT substrate under pulsed electric fields.^{27,28} However, Fig. 2(b) shows that the remanent strain is negligible after the removal of the electric fields in the continuous mode. This therefore suggests that one can easily obtain considerable remanent strain using the pulsed mode and that further nonvolatile control of the magnetic properties can be obtained through strain-mediated magnetoelectric coupling.

We then used the pulsed mode shown in Fig. 2(c) to control the AHE electrically. Under the optimum magnetic field bias of 100 Oe, the Hall resistivity versus pulsed electric field was measured as shown in Fig. 3(a). The criterion for the optimum bias magnetic field can be found in Fig. S2 (see supplementary material). At first, the Hall resistivity was approximately $1.35 \times 10^{-7} \Omega \text{ cm}$ at 0 kV/cm after negative full polarization (approximately -5.5 kV/cm). The Hall resistivity then decreased to $1.09 \times 10^{-7} \Omega \text{ cm}$ at 0 kV/cm after positive full polarization (approximately $+5.5$ kV/cm). The Hall resistivity change, which is defined as $[\rho_H(E) - \rho_H(0, \text{low})]/\rho_H(0, \text{low})$, ranges up to $\sim 23.9\%$ under electric fields at a magnetic field of 100 Oe. Here, $\rho_H(E)$ is the Hall resistivity at the electric field E and $\rho_H(0, \text{low})$ represents the lower resistivity at 0 kV/cm. This change is

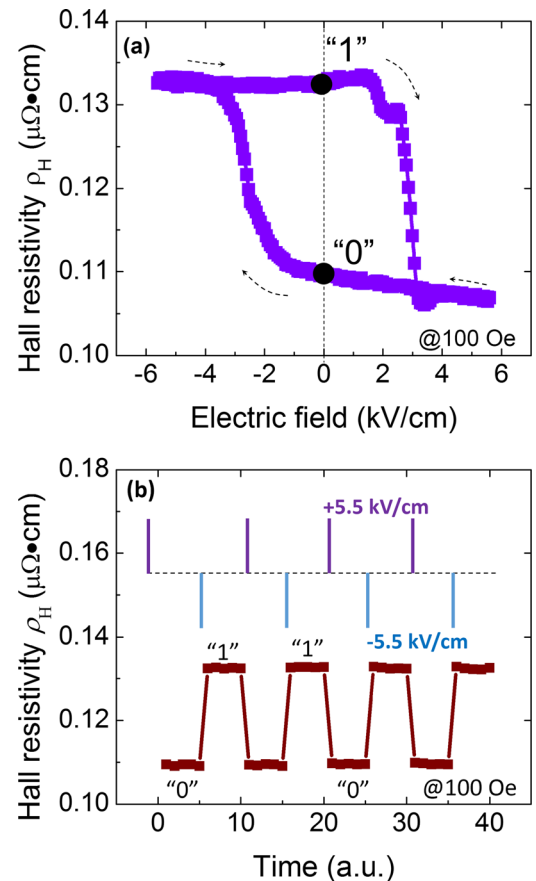


FIG. 3. (a) Electric-field control of the Hall voltage in the FePt-PMN-PT multiferroic heterostructure at 100 Oe using electric field amplitudes of +5.5 and -5.5 kV/cm. (b) Reversible electric-field control of the nonvolatile Hall resistivity using a sequence of pulsed electric fields under 100 Oe magnetic field bias.

comparable with that ($\sim 45\%$) obtained in $\text{Ni}_{43}\text{Mn}_{41}\text{Co}_5\text{Sn}_{11}/\text{PMN-PT}$ multiferroic heterostructures at 3 kV/cm and 5 kOe .¹⁸ Second, remanent Hall resistivities are also expected based on the remanent strain states that occur in the FePt thin films, as noted above. The low and high Hall resistance states are labeled “0” and “1” in Fig. 3(a) and correspond to the remanent strain states “A” and “B” shown in Fig. 2(d), respectively. The Hall resistivity can thus be modulated in a nonvolatile manner using pulsed electric fields.

To encode binary information via electric-field control of the AHE, a sequence of pulsed fields with amplitudes of $+5.5\text{ kV/cm}$ and -5.5 kV/cm is used as shown at the top of Fig. 3(b). On the one hand, the low Hall resistance state (encoded as “0”) and the high Hall resistance state (encoded as “1”), as labeled at the bottom of Fig. 3(b), are synchronously and reversibly switched during the repeated application of the electric field pulses of $+5.5$ and -5.5 kV/cm . On the other hand, both the low and high Hall resistance states are nonvolatile and remain upon removal of the pulsed electric fields because of the nonvolatile remanent strains that are present in the FePt thin films, in a manner similar to the nonvolatile resistance states that occur in $(011)\text{-La}_{2/3}\text{Sr}_{1/3}\text{MnO}_3/0.7\text{Pb}(\text{Mg}_{1/3}\text{Nb}_{2/3})\text{O}_3\text{-}0.3\text{PbTiO}_3$ multiferroic heterostructures.²⁷ Consequently, using a sequence of pulsed electric fields, the Hall resistivity can be reversibly modulated in a nonvolatile manner at room temperature, which indicates a promising approach for the development of memory devices.

To illustrate the strain-mediated magnetoelectric coupling mechanism in the FePt/PMN-PT multiferroic heterostructures, the magnetic states under the application of electrical (or strain) and magnetic fields are illustrated in Fig. 4. Based on the magnetic hysteresis loop measurements of the unpatterned FePt thin films [see Fig. S3(a) and S3(b) in the [supplementary material](#) and our previous work²¹], the FePt thin films are known to have in-plane magnetocrystalline anisotropy (independent of the in-plane direction in the polycrystal FePt thin film), while the out-of-plane axis is the magnetic hard axis due to the demagnetization field. In the patterned FePt thin films with a Hall bar geometry, the shape anisotropy or demagnetization field introduces an easy axis along the length direction of the Hall bar (see Fig. S3(c) in the [supplementary material](#)). Thus, the magnetization (or moment) favors alignment along the channel direction^{28,29} (or mainly along the x -axis, as shown in Fig. 4) in the absence of an external magnetic field (see Fig. S3(d) in the [supplementary material](#)). Figure 4(a) shows the magnetic state of the FePt Hall channel when it is depolarized from -5.5 kV/cm to 0 kV/cm at a bias of 100 Oe . The bias magnetic field \mathbf{H} tilts the magnetization \mathbf{M} towards the out-of-plane direction, as shown in Fig. 4(a). The resulting magnetization component M_z is thus oriented along the \mathbf{H} direction. Under the application of a $+5.5\text{ kV/cm}$ pulsed electric field, the remanent strain is induced in the FePt thin films as shown in Fig. 4(b), and this introduces an additional magnetoelastic energy F_{me} . Since the piezo-strain in the (001) -oriented PMN-PT substrate is uniformly biaxial, the shear strain is neglected here. Thus, F_{me} can be determined as follows:^{30,31}

$$F_{me} = -\frac{3}{2}\lambda_s Y \varepsilon_{xx} \cos^2 \varphi \sin^2 \theta, \quad (1)$$

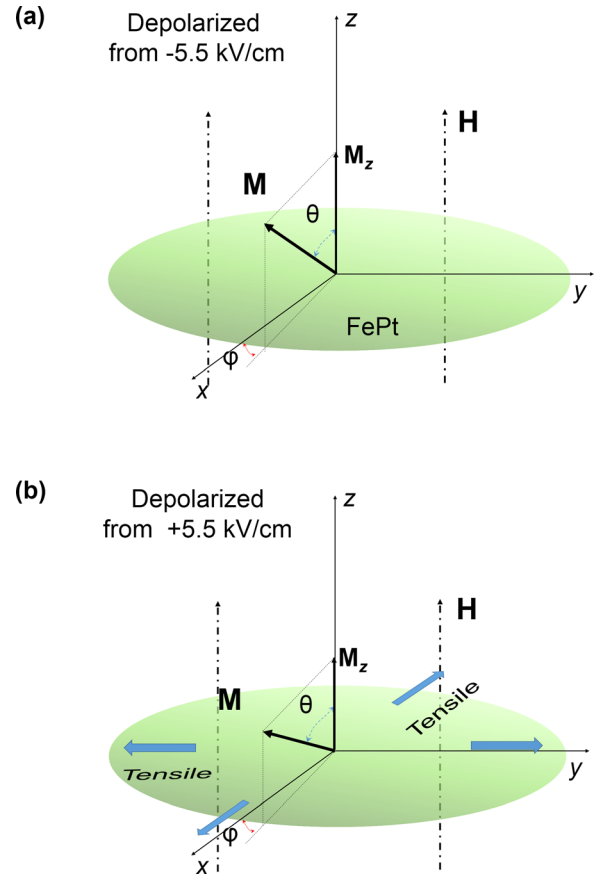


FIG. 4. Schematic illustration of the mechanism for electric-field control of the Hall effect via strain-mediated magnetoelectric coupling. (a) and (b) The magnetization states after depolarization from -5.5 kV/cm and $+5.5\text{ kV/cm}$, respectively. The magnetic field \mathbf{H} was set at 100 Oe . Tensile strain was formed as indicated by the blue arrows.

where λ_s is the magnetostriction constant (approximately $+70\text{ ppm}$),³² ε_{xx} is the in-plane strain, and Y is the Young’s modulus (>0) of the FePt thin film. When the electric field is reduced from -5.5 kV/cm to 0 kV/cm , the remanent strain is approximately $+120\text{ ppm}$, and thus, F_{me} is negative. This means that magnetization \mathbf{M} is not favorable along the out-of-plane direction from the free energy viewpoint of Eq. (1). Therefore, the magnetization \mathbf{M} will rotate from the out-of-plane direction towards the in-plane direction, as shown in Fig. 4(b). Consequently, M_z is weakened by the pulsed electric field, and this is in good agreement with previously reported results.^{14,29,33} Álvarez *et al.* demonstrated experimentally that the in-plane magnetization is enhanced by internal strain in the FePt thin films within a specific thickness range.²⁹ Magnetization reversal from the out-of-plane direction towards the in-plane direction under the application of electric fields was also observed to occur in $(\text{Co/Pt})_3/\text{Pb}(\text{Mg}_{1/3}\text{Nb}_{2/3})\text{O}_3\text{-PbTiO}_3$ multiferroic heterostructures through strain-mediated magnetoelectric coupling.^{14,33} The magnetic anisotropy of the FePt/PMN-PT multiferroic heterostructures under pulse electric fields is shown in Fig. S4 (see [supplementary material](#)).

We now consider how the AHE can be controlled using electric fields. It is well known that the empirical relationship among ρ_H , H_z , and M_z for the AHE is given by³⁴

$$\rho_H = R_0 H_z + R_s M_z, \quad (2)$$

where R_0 is the ordinary Hall coefficient, while R_s is the spontaneous anomalous Hall coefficient, which is dependent on various material-specific parameters.³⁴ M_z is the magnetization along the H_z direction. The term R_0H_z is usually several orders of magnitude smaller than the term R_sM_z and can thus be neglected. The AHE resistivity is therefore mainly dependent on the term R_sM_z and is thus proportional to M_z .^{21,22} In the remanent strain state “A,” as shown in Fig. 4(b), the out-of-plane magnetization M_z (marked in red) is weakened by the application of the positive pulsed electric fields. Consequently, the AHE resistivity is reduced and the low Hall resistance state of “0” is created by the positive electric fields. Using similar reasoning, it is possible to switch to the high Hall resistance state of “1” from the lower state by the application of negative electric fields. It should be mentioned that the electric field is an indirect approach here to control the AHE. Actually, the electric-field-induced piezo-strain from the ferroelectric PMN-PT modulates the magnetic states in the FePt thin film, and thus, the AHE is controlled indirectly by an electric field.

In summary, we have used electric fields to control the anomalous Hall effect in multiferroic FePt/PMN-PT hybrid heterostructures at room temperature. Using a sequence of pulsed electric fields, we first achieved the nonvolatile remanent strain states. Then, we observed a very high AHE tunability of up to 23.9% under the application of pulsed electric fields. The corresponding low- and high-Hall resistance states were created, and they were shown to be nonvolatile upon removal of the applied electric fields. A programmed pulsed electric field sequence can deterministically switch between the low- and high-Hall resistance states reversibly in a nonvolatile manner, thus enabling encoding of binary information. The observed behavior is the result of strain-mediated magnetoelectric coupling in the FePt/PMN-PT multiferroic heterostructures. Our approach is simple, effective, and nonvolatile and consumes little power. Therefore, EF controlled AHE using multiferroic heterostructures is another potentially viable implementation of spintronic random-access memory technologies.

See [supplementary material](#) for the crystalline phase of the FePt thin films, magnetic hysteresis curves of the FePt thin films, the criterion for the optimum magnetic field used in this work, and qualitative results for the magnetic anisotropy of the FePt thin films under pulse electric fields.

This work was supported in part by the Natural Science Foundation of China (51402281, 11775224, and 11504358) and the National Key Research and Development Program of China [2016YFA0300102 and 2016YFA0300103]. The work at Hefei University of Technology was partially supported by an internal research fund (407-0371000022). Work at Brown University was supported by the National Science Foundation (Grant No. DMR-1307056).

¹C. Song, B. Cui, F. Li, X. Zhou, and F. Pan, *Prog. Mater. Sci.* **87**, 33 (2017).

²E. De Ranieri, P. E. Roy, D. Fang, E. K. Vehstedt, A. C. Irvine, D. Heiss, A. Casiraghi, R. P. Campion, B. L. Gallagher, T. Jungwirth, and J. Wunderlich, *Nat. Mater.* **12**, 808 (2013).

³T. Maruyama, Y. Shiota, T. Nozaki, K. Ohta, N. Toda, M. Mizuguchi, A. A. Tulapurkar, T. Shinjo, M. Shiraishi, S. Mizukami, Y. Ando, and Y. Suzuki, *Nat. Nanotechnol.* **4**, 158 (2009).

⁴M. Liu, J. Lou, S. Li, and N. X. Sun, *Adv. Funct. Mater.* **21**, 2593 (2011).

⁵H. Ohno, D. Chiba, F. Matsukura, T. Omiya, E. Abe, T. Dietl, Y. Ohno, and K. Ohtani, *Nature* **408**, 944 (2000).

⁶R. H. Liu, W. L. Lim, and S. Urazhdin, *Phys. Rev. B* **89**, 220409(R) (2014).

⁷R. Gao, C. Fu, W. Cai, G. Chen, X. Deng, H. Zhang, J. Sun, and B. Shen, *Sci. Rep.* **6**, 20330 (2016).

⁸D. D. Awschalom and M. E. Flatté, *Nat. Phys.* **3**, 153 (2007).

⁹P. Li, A. Chen, D. Li, Y. Zhao, S. Zhang, L. Yang, Y. Liu, M. Zhu, H. Zhang, and X. Han, *Adv. Mater.* **26**, 4320 (2014).

¹⁰X. Yang, Z. Zhou, T. Nan, Y. Gao, G. M. Yang, M. Liu, and N. X. Sun, *J. Mater. Chem. C* **4**, 234 (2016).

¹¹Q. Zhang, Y. Yang, R. Gao, W. Zhou, Q. Li, D. Wang, and Y. Du, *Mater. Lett.* **121**, 50 (2014).

¹²A. Ahlawat, S. Satapathy, R. J. Choudhary, M. K. Singh, and P. K. Gupta, *Mater. Lett.* **181**, 123 (2016).

¹³Q. Li, A. Tan, A. Scholl, A. T. Young, M. Yang, C. Hwang, A. T. N'Diaye, E. Arenholz, J. Li, and Z. Q. Qiu, *Appl. Phys. Lett.* **110**, 262405 (2017).

¹⁴B. Peng, Z. Zhou, T. Nan, G. Dong, M. Feng, Q. Yang, X. Wang, S. Zhao, D. Xian, Z.-D. Jiang, W. Ren, Z.-G. Ye, N. X. Sun, and M. Liu, *ACS Nano* **11**, 4337 (2017).

¹⁵H. Sohn, M. E. Nowakowski, C.-y. Liang, J. L. Hockel, K. Wetzlar, S. Keller, B. M. McLellan, M. A. Marcus, A. Doran, A. Young, M. Kläui, G. P. Carman, J. Bokor, and R. N. Candler, *ACS Nano* **9**, 4814 (2015).

¹⁶A. K. Biswas, H. Ahmad, J. Atulasimha, and S. Bandyopadhyay, *Nano Lett.* **17**, 3478 (2017).

¹⁷K. Cai, M. Yang, H. Ju, S. Wang, Y. Ji, B. Li, K. W. Edmonds, Y. Sheng, B. Zhang, N. Zhang, S. Liu, H. Zheng, and K. Wang, *Nat. Mater.* **16**, 712 (2017).

¹⁸S. Y. Chen, Y. X. Zheng, Q. Y. Ye, H. C. Xuan, Q. Q. Cao, Y. Deng, D. H. Wang, Y. W. Du, and Z. G. Huang, *J. Alloys Compd.* **509**, 8885 (2011).

¹⁹S. M. Wu, S. A. Cybart, P. Yu, M. D. Rossell, J. X. Zhang, R. Ramesh, and R. C. Dynes, *Nat. Mater.* **9**, 756 (2010).

²⁰C. Feng, J. Zhao, F. Yang, K. Gong, S. Hao, Y. Cao, C. Hu, J. Zhang, Z. Wang, L. Chen, S. Li, L. Sun, L. Cui, and G. Yu, *Sci. Rep.* **6**, 20199 (2016).

²¹Q. Hao, W. Chen, S. Wang, and G. Xiao, *J. Appl. Phys.* **122**, 033901 (2017).

²²G. X. Miao and G. Xiao, *Appl. Phys. Lett.* **85**, 73 (2004).

²³C. L. Canedy, G. Q. Gong, J. Q. Wang, and G. Xiao, *J. Appl. Phys.* **79**, 6126 (1996).

²⁴X. Xue, Z. Zhou, B. Peng, M. Zhu, Y. Zhang, W. Ren, T. Ren, X. Yang, T. Nan, N. X. Sun, and M. Liu, *Sci. Rep.* **5**, 16480 (2015).

²⁵B. Hong, Y. Yang, J. Zhao, K. Hu, J. Peng, H. Zhang, W. Liu, Z. Luo, H. Huang, X. Li, and C. Gao, *Mater. Lett.* **169**, 110 (2016).

²⁶Y. Yang, M. M. Yang, Z. L. Luo, H. Huang, H. Wang, J. Bao, C. Hu, G. Pan, Y. Yao, Y. Liu, X. G. Li, S. Zhang, Y. G. Zhao, and C. Gao, *Appl. Phys. Lett.* **100**, 043506 (2012).

²⁷Y. Yang, Z. L. Luo, M. M. Yang, H. Huang, H. Wang, J. Bao, G. Pan, C. Gao, Q. Hao, S. Wang, M. Jokubaitis, W. Zhang, G. Xiao, Y. Yao, Y. Liu, and X. G. Li, *Appl. Phys. Lett.* **102**, 033501 (2013).

²⁸L. Yang, Y. Zhao, S. Zhang, P. Li, Y. Gao, Y. Yang, H. Huang, P. Miao, Y. Liu, A. Chen, C. Nan, and C. Gao, *Sci. Rep.* **4**, 4591 (2014).

²⁹N. R. Álvarez, J. E. Gómez, A. E. Moya Riffo, M. A. V. Álvarez, and A. Butera, *J. Appl. Phys.* **119**, 083906 (2016).

³⁰M. Liu, O. Obi, J. Lou, Y. Chen, Z. Cai, S. Stoute, M. Espanol, M. Lew, X. Situ, K. S. Ziemer, V. G. Harris, and N. X. Sun, *Adv. Funct. Mater.* **19**, 1826 (2009).

³¹B. Bagyalakshmi, M. V. GajendraBabu, B. Sundarakannan, S. Kalavathi, V. Sridharan, and G. Amarendra, *Mater. Lett.* **170**, 48 (2016).

³²J. A. Aboaf, T. R. McGuire, S. R. Herd, and E. Klokholm, *IEEE Trans. Magn.* **20**, 1642 (1984).

³³Y. Sun, Y. Ba, A. Chen, W. He, W. Wang, X. Zheng, L. Zou, Y. Zhang, Q. Yang, L. Yan, C. Feng, Q. Zhang, J. Cai, W. Wu, M. Liu, L. Gu, Z. Cheng, C.-W. Nan, Z. Qiu, Y. Wu, J. Li, and Y. Zhao, *ACS Appl. Mater. Interfaces* **9**, 10855 (2017).

³⁴N. Nagaosa, J. Sinova, S. Onoda, A. H. MacDonald, and N. P. Ong, *Rev. Mod. Phys.* **82**, 1539 (2010).